ELSEVIER

Journal of Chromatography A, 702 (1995) 45–57

JOURNAL OF CHROMATOGRAPHY A

"Perfusion chromatography". The effects of intra-particle convective velocity and microsphere size on column performance

A.I. Liapis*, Y. Xu, O.K. Crosser, A. Tongta

Department of Chemical Engineering and Biochemical Processing Institute, University of Missouri–Rolla, Rolla, MO 65401-0249, USA

Abstract

A mathematical model describing the dynamic adsorption in columns with spherical bidisperse perfusive or spherical bidisperse purely diffusive adsorbent particles is presented and its solution is obtained numerically. The adsorption of bovine serum albumin on spherical anion-exchange porous particles was studied for different values of the intraparticle Peclet number, Pe_{intra}, and of the microsphere diameter, d_m. The results show a departure from spherical symmetry of the isoconcentration profiles of the adsorbate in the porous adsorbent particle as Pe_{intra} increases. This spherical asymmetry increases the adsorbate availability in the pore fluid of the macroporous region and also increases the concentration of the adsorbate in the adsorbed phase in the upstream half of the spherical adsorbent particle. If, for example, the concentration profiles of the adsorbate in the adsorbed phase of the porous adsorbent particles could be determined experimentally and if these profiles show a departure from spherical symmetry, then this result could suggest that the porous adsorbent particles may have exhibited perfusion behavior under the conditions of operation of the column. The dynamic percentage utilization of the adsorptive capacity of the column increases as Pe_{intra} increases and d_m decreases. The percentage breakthrough to be selected for column switching is influenced by the magnitude of Pe_{intra} because of its effect on the dynamic percentage utilization of the adsorptive capacity of the column.

1. Introduction

The separation process that involves the flow of a liquid phase through the through-pores of porous chromatographic particles packed in a column [1–5] has been called by Afeyan et al. [1] "perfusion chromatography". This term "perfusion chromatography" is often not defined with precision. In this work, as in previous publications [2–5], we define "perfusion chromatography" as referring to any chromatographic system in which the intraparticle convective velocity, v_p, is non-zero [1–5].

Liapis and McCoy [4] considered that the perfusive adsorbent particles with a bidisperse [4] porous structure have a macroporous region made by the through-pores [1,2,4,5] in which intraparticle convection and pore diffusion occur, and a microporous [4] region made by spherical microparticles (microspheres [1]) that

* Corresponding author.

0021-9673/95/$09.50
SSDI 0021-9673(94)01022-6

are taken to be purely diffusive. In this work, a mathematical model that could describe adsorption in columns having spherical perfusive adsorbent particles with a bidisperse porous structure is presented. The model is then solved and used to study the dynamic behavior of a column system involving the adsorption of bovine serum albumin (BSA) on spherical anion-exchange porous particles.

2. Mathematical model

Adsorption is considered to take place from a flowing liquid stream in a fixed bed of spherical perfusive adsorbent particles of bidisperse porous structure under isothermal conditions. The differential mass balance for the adsorbate in the flowing fluid stream gives [2–4]

$$\frac{\partial C_d}{\partial t} - D_L \cdot \frac{\partial^2 C_d}{\partial x^2} + \frac{V_f}{\varepsilon} \cdot \frac{\partial C_d}{\partial x} = -\frac{(1-\varepsilon)}{\varepsilon} \frac{\partial \bar{C}_{ps}}{\partial t} \tag{1}$$

The initial and boundary conditions of Eq. (1) are as follows:

$$\text{at } t = 0: \quad C_d = 0, \quad 0 \leq x \leq L \tag{2}$$

$$\text{at } x = 0: \quad \frac{V_f}{\varepsilon} \cdot C_d\Big|_{x=0} - D_L \cdot \frac{\partial C_d}{\partial x}\Big|_{x=0} = \frac{V_f}{\varepsilon} \cdot C_{d,in}, \quad t > 0 \tag{3}$$

$$\text{at } x = L: \quad \frac{\partial C_d}{\partial x}\Big|_{x=L} = 0, \quad t > 0 \tag{4}$$

The value of $C_{d,in}$ may be constant or it may vary with time. An expression for estimating D_L was presented by Arnold et al. [6], but in certain systems the axial dispersion is so low that by setting its value equal to zero the error introduced in the prediction of the behavior of an affinity adsorption system is not significant [6,7]. When the axial dispersion coefficient is set equal to zero, Eq. 3 (with $D_L = 0$) becomes as follows:

$$\text{at } x = 0: \quad C_d = C_{d,in}, \quad t > 0 \tag{5}$$

The spherical perfusive adsorbent particles with a bidisperse [4] porous structure are considered to have a microporous [4] region made by spherical microparticles (microspheres [1]) that are taken to be purely diffusive, and a macroporous [4] region made by the through-pores [1,2,4,5] in which intraparticle convention and pore diffusion occur. Liapis and McCoy [4] were first in proposing the above representation for the bidisperse perfusive adsorbent particles and in modeling the mass transfer mechanisms in the macroporous and microporous regions of the bidisperse perfusive adsorbent particles. The mass transfer mechanisms in the macroporous and microporous regions are presented on p. 86 of Ref. [4]. In Fig. 1, a diagram of a spherical perfusive adsorbent particle with a bidisperse porous structure is shown; x_1 represents the axial coordinate for the spherical perfusive adsorbent particle and is parallel to the axial coordinate x of the column.

The differential mass balance for the adsorbate in the macroporous region of a perfusive adsorbent particle of spherical geometry is given by

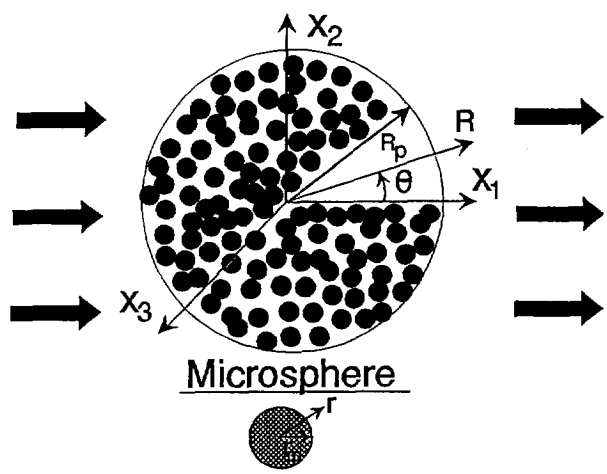

Fig. 1. Spherical perfusive adsorbent particle with a bidisperse porous structure (the arrows indicate the direction of fluid flow). R_p = Radius of perfusive particle; r_m = radius of microsphere.

$$\varepsilon_p \cdot \frac{\partial C_p}{\partial t} + \varepsilon_p v_{pR} \cdot \frac{\partial C_p}{\partial R} + \varepsilon_p v_{p\theta}\left(\frac{1}{R}\right)\frac{\partial C_p}{\partial \theta} + (1-\varepsilon_p)\frac{\partial \bar{C}_s}{\partial t} = \varepsilon_p D_p\left[\left(\frac{1}{R^2}\right)\frac{\partial}{\partial R}\left(R^2 \cdot \frac{\partial C_p}{\partial R}\right) + \left(\frac{1}{R^2 \sin\theta}\right)\frac{\partial}{\partial \theta}\left(\sin\theta \cdot \frac{\partial C_p}{\partial \theta}\right)\right] \quad (6)$$

The variables v_{pR} and $v_{p\theta}$ represent the intraparticle velocity components along the R and θ directions, respectively. Neale et al. [8] obtained analytical expressions for the stream functions outside and inside the permeable spheres. By using the expression of Neale et al. [8] for the stream function inside the particle, the following equations for v_{pR} and $v_{p\theta}$ are obtained:

$$v_{pR} = V_f \cos\theta\left[F - \left(\frac{H}{\xi^2}\right)\left(\frac{\sinh\xi}{\xi} - \cosh\xi\right)\right] \quad (7)$$

$$v_{p\theta} = -V_f \sin\theta\left\{F - \left(\frac{H}{2\xi}\right)\left[\left(\frac{\xi\cosh\xi - \sinh\xi}{\xi^2}\right) - \sinh\xi\right]\right\} \quad (8)$$

Neale et al. [8] reported the expressions for ξ, F and H, which are as follows:

$$\xi = \frac{R}{\sqrt{K_p}} \quad (9)$$

$$F = \frac{B}{\beta^3} + 10D \quad (10)$$

$$H = \frac{1}{J}\left[6\beta^2(\operatorname{sech}\beta)(1-\eta^5)\right] \quad (11)$$

where

$$\beta = \frac{R_p}{\sqrt{K_p}} \quad (12)$$

$$\eta = (1-\varepsilon)^{1/3} \quad (13)$$

$$J = 2\beta^2 - 3\beta^2\eta + 3\beta^2\eta^5 - 2\beta^2\eta^6 + 90\beta^{-2}\eta^5 + 42\eta^5 - 30\eta^6 + 3 - \frac{\tanh\beta}{\beta}(-3\beta^2\eta + 15\beta^2\eta^5 - 12\beta^2\eta^6 + 90\beta^{-2}\eta^5 + 72\eta^5 - 30\eta^6 + 3) \quad (14)$$

$$B = \frac{1}{J}\left[3\beta^3 + 2\beta^3\eta^5 + 30\beta\eta^5 - \frac{\tanh\beta}{\beta}(3\beta^3 + 12\beta^3\eta^5 + 30\beta\eta^5)\right] \quad (15)$$

$$D = -\frac{\eta^5 A}{\beta^5} \quad (16)$$

$$A = \frac{1}{J}\left[\beta^5 + 6\beta^3 - \frac{\tanh\beta}{\beta}(3\beta^5 + 6\beta^3)\right] \quad (17)$$

The value of the particle permeability, K_p, in Eqs. 9 and 12 depends on the diameter of the microspheres, d_m, the porosity of the macroporous region, ε_p, and on the pore-size distribution of the macroporous region. The pore-size distribution of the macroporous region depends on the process employed to aggregate the microspheres to construct the spherical perfusive particle. As a first approximation, the value of K_p could be estimated from the expressions for K_p reported in Refs. [9–11]. The axial component of the intraparticle velocity, v_{px_1}, which is parallel to the flowing fluid stream along the axis of the column, is given by

$$v_{px_1} = v_{pR}\cos\theta - v_{p\theta}\sin\theta \quad (18)$$

The initial and boundary conditions of Eq. 6 are as follows:

at $t = 0$: $C_p = 0$, $0 \le R \le R_p$ (19)

at $R = R_p$: $C_p = C_d$, $t > 0$, $0 \le \theta \le \pi$ (20)

at $R = 0$: C_p = finite, $t > 0$, $0 \le \theta \le \pi$ (21)

at $\theta = 0$: $\left.\frac{\partial C_p}{\partial \theta}\right|_{\theta=0} = 0$, $0 \le R \le R_p$ (22)

at $\theta = \pi$: $\left.\frac{\partial C_p}{\partial \theta}\right|_{\theta=\pi} = 0$, $0 \le R \le R_p$ (23)

The differential mass balance for the adsor-

bate in a purely diffusive spherical microparticle (microsphere) is given by [4]

$$\varepsilon_{pm}\cdot\frac{\partial C_{pm}}{\partial t}+\left(\frac{1}{1-\varepsilon_p}\right)\frac{\partial C_{sm}}{\partial t}=\varepsilon_{pm}D_{pm}\left(\frac{\partial^2 C_{pm}}{\partial r^2}+\frac{2}{r}\cdot\frac{\partial C_{pm}}{\partial r}\right) \quad (24)$$

The accumulation term, $\partial C_{sm}/\partial t$, of the adsorbed species can be quantified if a thermodynamically consistent mathematical model could be constructed that could describe the mechanism of adsorption for the adsorbate. For isothermal adsorption systems, the term $\partial C_{sm}/\partial t$ could be of the form

$$\frac{\partial C_{sm}}{\partial t}=f(C_{pm}, C_{sm}, \boldsymbol{k}) \quad (25)$$

where f represents the functional form of the dynamic adsorption mechanism for the adsorbate, and $\boldsymbol{k}$ represents the vector of the rate constants that characterize the interaction kinetics between the adsorbate molecules and the active sites. One well known form of Eq. 25 for single-component adsorption ($A + S \underset{k_2}{\overset{k_1}{\rightleftharpoons}} AS$) is as follows [2,4,12]:

$$\frac{\partial C_{sm}}{\partial t}=k_1 C_{pm}(C_T - C_{sm}) - k_2 C_{sm} \quad (26)$$

The term $\partial C_{sm}/\partial t$ in Eq. 24 could now be replaced by the right-hand side of Eq. 26. The initial and boundary conditions of Eqs. 24 and 25 (and also of Eq. 26) are considered to be as follows:

$$\text{at } t=0: \quad C_{pm}=0, \quad 0\le r\le r_m \quad (27)$$

$$\text{at } t=0: \quad C_{sm}=0, \quad 0\le r\le r_m \quad (28)$$

$$\text{at } r=r_m: \quad C_{pm}=C_p(t, R, \theta), \quad t>0 \quad (29)$$

$$\text{at } r=0: \quad \left.\frac{\partial C_{pm}}{\partial r}\right|_{r=0}=0, \quad t>0 \quad (30)$$

The variable $\bar{C}_s$ in Eq. 6 could be calculated from the following expression:

$$\bar{C}_s=\frac{3}{r_m^3}\left[\int_0^{r_m}\varepsilon_{pm}C_{pm}r^2\,dr+\int_0^{r_m}\left(\frac{1}{1-\varepsilon_p}\right)C_{sm}r^2\,dr\right] \quad (31)$$

The accumulation term $\partial\bar{C}_s/\partial t$ in Eq. 6 is obtained by differentiating Eq. 31 with respect to time, and hence

$$\frac{\partial\bar{C}_s}{\partial t}=\frac{3}{r_m^3}\left\{\frac{\partial}{\partial t}\left(\int_0^{r_m}\varepsilon_{pm}C_{pm}r^2\,dr\right)+\frac{\partial}{\partial t}\left[\int_0^{r_m}\left(\frac{1}{1-\varepsilon_p}\right)C_{sm}r^2\,dr\right]\right\} \quad (32)$$

For a given pair of values of R and θ, the average concentration of the adsorbate in the adsorbed phase, $\bar{C}_{sa}$, is obtained from the following expression:

$$\bar{C}_{sa}=(1-\varepsilon_p)\frac{3}{r_m^3}\left[\int_0^{r_m}\left(\frac{1}{1-\varepsilon_p}\right)C_{sm}r^2\,dr\right] \quad (33)$$

Finally, the term $\partial\bar{C}_{ps}/\partial t$ in Eq. 1 is given by

$$\frac{\partial\bar{C}_{ps}}{\partial t}=\frac{3}{2R_p^3}\left\{\frac{\partial}{\partial t}\left(\int_0^{\pi}\int_0^{R_p}\varepsilon_p C_p R^2\sin\theta\,dR\,d\theta\right)+\frac{\partial}{\partial t}\left[\int_0^{\pi}\int_0^{R_p}(1-\varepsilon_p)\bar{C}_s R^2\sin\theta\,dR\,d\theta\right]\right\} \quad (34)$$

since

$$\bar{C}_{ps}=\frac{3}{2R_p^3}\left\{\int_0^{\pi}\int_0^{R_p}[\varepsilon_p C_p+(1-\varepsilon_p)\bar{C}_s]R^2\sin\theta\,dR\,d\theta\right\} \quad (35)$$

The dynamic behavior of a column adsorption system involving spherical perfusive adsorbent particles with a bidisperse porous structure could be obtained by solving simultaneously Eqs. 1, 6, 24 and 25. It should be noted that Eq. 26 could be used for Eq. 25 with the understanding that Eq. 26 represents only one possible form of Eq. 25.

It should be mentioned that if the intraparticle velocity is zero ($v_{pR}=v_{p\theta}=0$), then the spherical adsorbent particles are considered to be purely

diffusive. In this case, the concentration C_p is considered to be independent of θ, and thus the term $\partial C_p/\partial\theta$ in Eq. 6 is taken to be equal to zero. Further, the boundary conditions given by Eqs. 22 and 23 are not needed, and the boundary condition at $R=0$ becomes $(\partial C_p/\partial R)|_{R=0} = 0$.

2.1. Numerical solution

The solution of the equations of the mathematical model presented in this work was obtained by employing (a) the method of orthogonal collocation [4,9,13,14] on the space variable r of the continuity equation of the adsorbate in the microparticle, (b) the double collocation [13,15] method on the space variables R and θ of the continuity equation of the adsorbate in the macroporous region (through-pores) and (c) the method of orthogonal collocation on finite elements [4,9,13] on the space variable x of the continuity equation of the adsorbate in the flowing fluid stream in the column; the resulting non-linear ordinary differential equations were integrated by using Gear's method [14], which is employed in the LSODES component of the ODEPACK [16] software package.

3. Results and discussion

In this work, the dynamic behavior of a column system involving the adsorption of bovine serum albumin (BSA) into spherical anion-exchange porous particles was studied, for different values of the intraparticle Peclet number, Pe_{intra}, and of the microparticle (microsphere) diameter, d_m. The diameter of the adsorbent particles, d_p, was taken to be $1.5\cdot10^{-5}$ m, and three different values for the diameter of the microparticles, d_m, were employed: $7.13\cdot10^{-8}$, $7.13\cdot10^{-7}$ and $7.13\cdot10^{-6}$ m. If the intraparticle Peclet number, Pe_{intra}, could be defined as

$$Pe_{intra} = \frac{v_{px_1} d_p}{D_p} \tag{36}$$

then, from Eqs. 7, 8 and 18, it is apparent that the value of v_{px_1}, and hence the value of Pe_{intra}, depends on the values of R and θ considered in the evaluation of v_{px_1}. The value of v_{px_1} becomes independent of the values of R and θ when $H=0$ in Eqs. 7 and 8. For purely diffusive adsorbent particles $Pe_{intra}=0$, whereas for adsorbent particles with non-zero intraparticle fluid flow $Pe_{intra}>0$. In Table 1, the values of the parameters used for the dynamic simulations of the adsorption system studied in this work are presented. The values of other parameters are reported in the captions of the figures. It should be mentioned that the value of C_T in Table 1 represents the largest (maximum) amount of BSA that could be adsorbed per unit volume of the adsorbent particle. Further, the value of $C_{d,in}=0.1$ kg/m^3 in Table 1 indicates that the value of the inlet concentration of the adsorbate in the flowing fluid stream remains constant for all times of the adsorption stage (that is, the value of $C_{d,in}$ in the boundary condition given by Eq. 5 remains constant and equal to 0.1 kg/m^3 for all times), and this indicates that the simulation studies of this work examine systems of frontal analysis.

The values of the parameters of the system studied are such that the value of H in Eqs. 7 and 8 is essentially equal to zero. Thus, the values of v_{pR}, $v_{p\theta}$ and v_{px_1}, for the adsorption system studied, are obtained from the following expressions:

$$v_{pR} \approx FV_f \cos\theta \tag{37}$$

$$v_{p\theta} \approx -FV_f \sin\theta \tag{38}$$

$$v_{px_1} = FV_f \tag{39}$$

In this case, the expression for the intraparticle Peclet number when using Eq. 36 is

Table 1
Values of the parameters of the column system involving the adsorption of BSA on spherical anion-exchange porous adsorbent particles

$C_{d,in}=0.1$ kg/m^3; $C_T=78.3$ kg/m^3; $d_p=1.5\cdot10^{-5}$ m;
$\varepsilon=0.35$; $\varepsilon_p=0.13$; $\varepsilon_{pm}=0.48$; $T=296$ K;
$D_p=3.835\cdot10^{-12}$ m^2/s, $D_{pm}=7.08\cdot10^{-12}$ m^2/s, $D_L=0$;
$K=k_1/k_2=8.026$ m^3/kg; $k_1=1.05$ m^3/kg·s;
$k_2=0.131$ s^{-1}; $L=0.1$ m, $V_f=2.778\cdot10^{-3}$ m/s

$$Pe_{intra} = \frac{v_{px} d_p}{D_p} = \frac{(FV_t) d_p}{D_p} \quad (40)$$

In this work, the Pe_{intra} given by Eq. 40 was varied between 0 and 150.

The numerical solution of the mathematical model presented in the previous section allows the determination of intraparticle concentration profiles of the adsorbate in the pore fluid and in the adsorbed phase, and also the determination of transport rates and the dynamic performance of the adsorption system for a variety of adsorbent particle characteristics and operating conditions of the column. Some sample calculations of the adsorption of BSA into spherical anion-exchange porous particles are presented for the purpose of illustrating certain important features of the adsorption system in the presence of intraparticle fluid flow.

In Figs. 2a–7a, the dimensionless isoconcentration profiles of the adsorbate in the pore fluid of the pores of the macroporous region of the adsorbent particle are presented, and in Figs. 2b–7b the dimensionless isoconcentration profiles of the adsorbate in the adsorbed phase of the absorbent particle are shown. In Figs. 2–7 the outermost contours represent the isoconcentrations at the surface ($R = R_p$) of the particle, and the data in Figs. 2–7 were obtained for the position in the column located at $x = 0.125L$ and at time $t = 60$ min.

The effect of increasing Pe_{intra} is clearly shown through the change in the symmetry of the concentration profiles of the adsorbate in the adsorbent particle. Examination of the concentration contours of Figs. 2 and 5, for $Pe_{intra} = 0$ and 5, respectively, shows that there is a departure from spherical symmetry of the concentration profiles of the adsorbate as Pe_{intra} increases. As Pe_{intra} increases, the smallest concentration moves downstream, and hence there is higher adsorbate availability in the pore fluid of the macroporous region and a higher concentration of adsorbate in the adsorbed phase in the upstream half of the sphere than the downstream half. This is due to the intraparticle fluid flow mechanism operating in the same direction as pore diffusion in the upstream part of the absorbent particle but opposite to the pore diffusion mechanism downstream. Further, the fluid moving by intraparticle convection to the downstream part of the adsorbent particle has limited adsorbate content as most of the adsorbate was already adsorbed upstream. The results in Figs. 2–7 also show that the magnitude of the departure from spherical symmetry of the con-

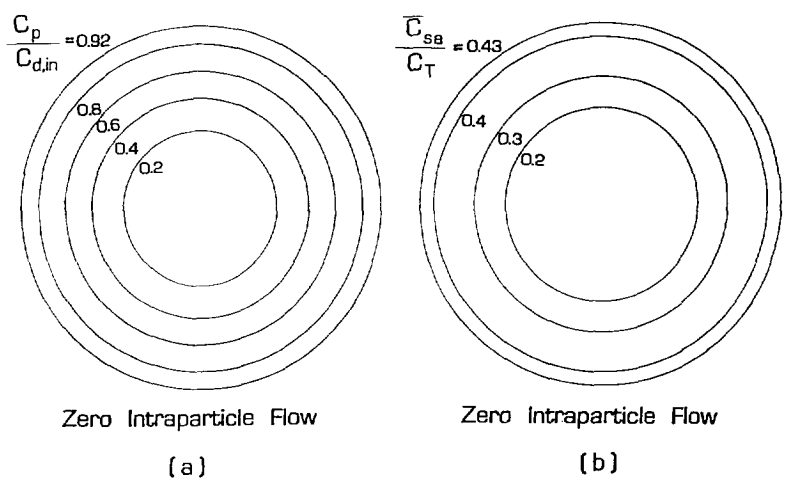

Fig. 2. Isoconcentration contours of the concentration of the adsorbate in the pore fluid of the macroporous region and in the adsorbed phase of the porous adsorbent particle when $d_m = 7.13 \cdot 10^{-8}$ m and $Pe_{intra} = 0$, at $x = 0.125L$ and $t = 60$ min. (a) $C_p/C_{d,in}$; (b) $\bar{C}_{ss}/C_T$.

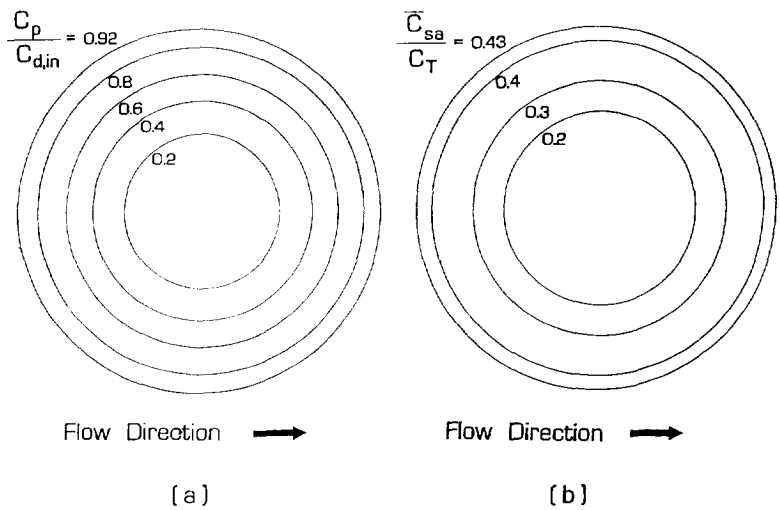

Fig. 3. Isoconcentration contours of the concentration of the adsorbate in the pore fluid of the macroporous region and in the adsorbed phase of the porous adsorbent particle when $d_m = 7.13 \cdot 10^{-7}$ m and $Pe_{intra} = 1$, at $x = 0.125L$ and $t = 60$ min. (a) $C_p/C_{d,in}$; (b) $\bar{C}_{sa}/C_T$.

centration profiles of the adsorbate increases as the magnitude of Pe_{intra} increases. Also, by comparing the results in Figs. 2 and 3 it can be observed that the differences in the concentration profiles are insignificant, whereas by comparing the results in Figs. 2 and 4 it becomes apparent that there are some slight differences between the concentration profiles. The data in Figs. 2–7 indicate that the beginning of an observable departure from spherical symmetry of the concentration profiles of the adsorbate occurs, for the adsorption system studied, for

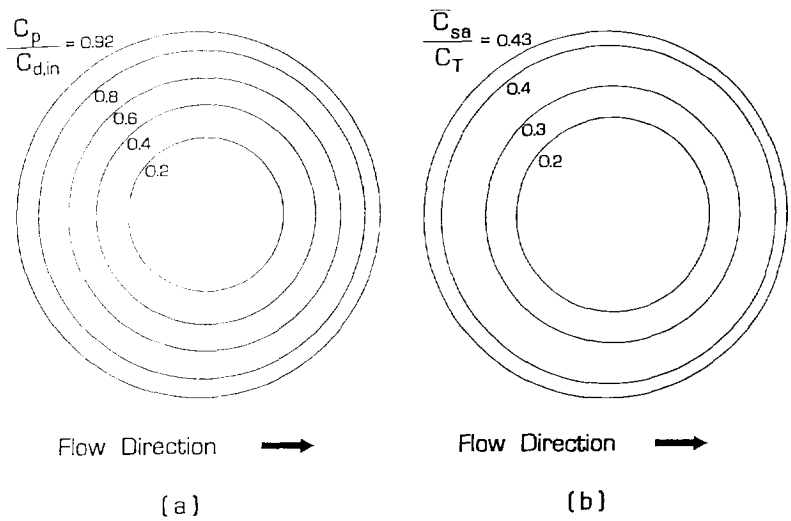

Fig. 4. Isoconcentration contours of the concentration of the adsorbate in the pore fluid of the macroporous region and in the adsorbed phase of the porous adsorbent particle when $d_m = 7.13 \cdot 10^{-7}$ m and $Pe_{intra} = 2$, at $x = 0.125L$ and $t = 60$ min. (a) $C_p/C_{d,in}$; (b) $\bar{C}_{sa}/C_T$.

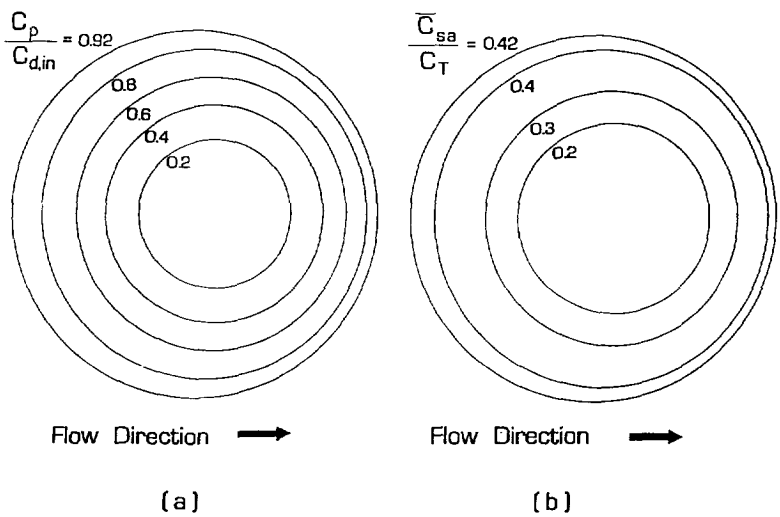

Fig. 5. Isoconcentration contours of the concentration of the adsorbate in the pore fluid of the macroporous region and in the adsorbed phase of the porous adsorbent particle when $d_m = 7.13 \cdot 10^{-8}$ m and $Pe_{intra} = 5$, at $x = 0.125L$ and $t = 60$ min. (a) $C_p/C_{d,in}$; (b) $\bar{C}_{sa}/C_T$.

values of $Pe_{intra} \geq 2$. It should also be mentioned that as Pe_{intra} increases and the adsorbate concentration minimum moves downstream, the overall adsorbate content of the spherical adsorbent particle increases; this was also the case when the porous adsorbent particle had slab [2,4] geometry. It is also worth mentioning that model simulations using the values of the parameters in Table 1, the values of the intraparticle Peclet numbers reported in the captions of Figs. 2–7 and considering the size of the microspheres to be either $d_m = 7.13 \cdot 10^{-7}$ or $7.13 \cdot 10^{-6}$ m, provided isoconcentration profiles whose behavior was similar to the behavior of the iso-

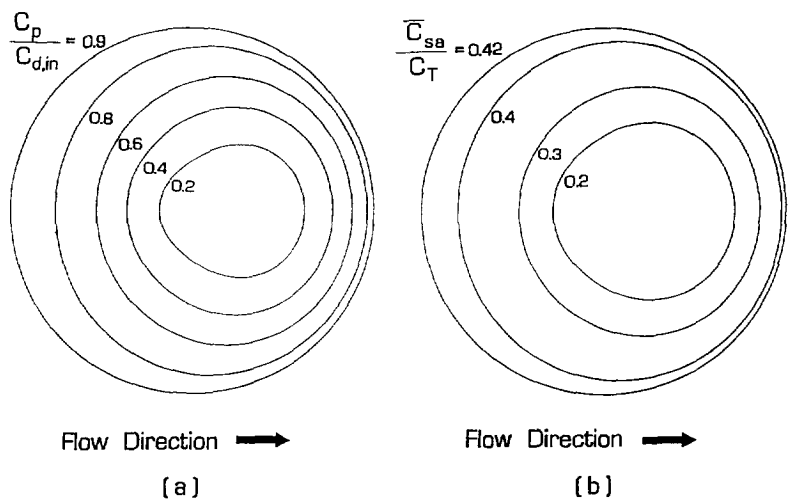

Fig. 6. Isoconcentration contours of the concentration of the adsorbate in the pore fluid of the macroporous region and in the adsorbed phase of the porous adsorbent particle when $d_m = 7.13 \cdot 10^{-8}$ m and $Pe_{intra} = 10$, at $x = 0.125L$ and $t = 60$ min. (a) $C_p/C_{d,in}$; (b) $\bar{C}_{sa}/C_T$.

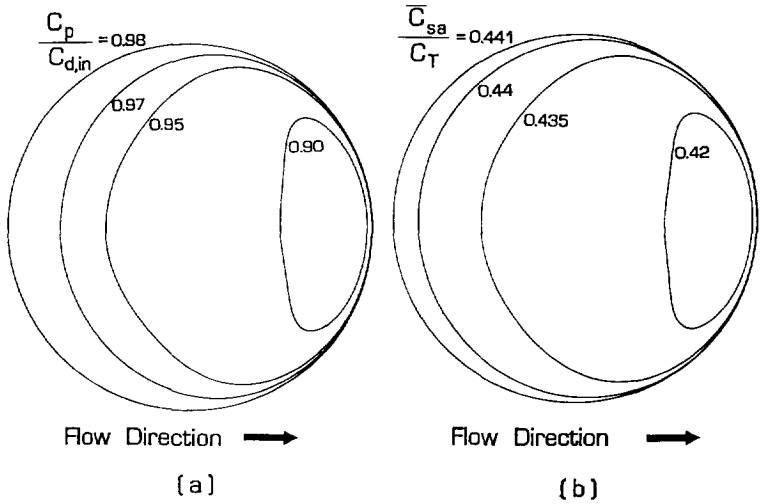

Fig. 7. Isoconcentration contours of the concentration of the adsorbate in the pore fluid of the macroporous region and in the adsorbed phase of the porous adsorbent particle when $d_m = 7.13 \cdot 10^{-8}$ m and $Pe_{intra} = 50$, at $x = 0.125L$ and $t = 60$ min. (a) $C_p/C_{d,in}$; (b) $\bar{C}_{sa}/C_T$.

concentration profiles presented in Figs. 2–7, as the value of the intraparticle Peclet number was being increased.

At this point, it may be useful to suggest that if the intraparticle convective velocity could not be measured experimentally for a given kind of chromatographic porous adsorbent particles, then the behavior of the results in Figs. 2–7 could be considered to provide an indirect test for determining if a given kind of chromatographic porous adsorbent particles could exhibit perfusion behavior when the column in which these particles are packed is operated under conditions of interest to the user. For instance, if it had been determined experimentally that the immobilized adsorption sites on the surface of the pores of the porous adsorbent particles were distributed evenly throughout the interior of the particles, then it might be possible to label the adsorbate molecules of the flowing fluid stream and determine experimentally the concentration profiles of the adsorbate molecules in the adsorbed phase of the chromatographic porous adsorbent particles taken from different axial positions of the bed, after the column was operated under conditions of interest to the user. If the experimentally determined concentration profiles of the adsorbate molecules in the adsorbed phase of the porous adsorbent particles show a departure from spherical symmetry, then this result could suggest that the chromatographic porous absorbent particles of the column may have exhibited perfusion behavior under the conditions of operation of the column.

In Table 2, the dynamic percentage utilization of the adsorptive capacity of the column at 1% and 10% breakthrough is presented. The total adsorptive capacity of the column is defined as the total amount of adsorbate in the adsorbed phase (in the column) at equilibrium (evaluated with respect to the value of $C_{d,in}$). The dynamic utilization of the adsorptive capacity of the column is defined as the ratio of the total amount of adsorbate in the adsorbed phase of the column when the desired breakthrough occurs to the total adsorptive capacity of the column. The dynamic percentage utilization of the adsorptive capacity of the column is obtained by multiplying the dynamic utilization of the adsorptive capacity of the column (defined above) by 100. The results in Table 2 show that for a given value of d_m, the dynamic percentage utilization of the adsorptive capacity of the column increases as the value of Pe_{intra} increases. Further, for a given value of Pe_{intra} the dynamic percentage utilization of the adsorptive capacity of the column

Table 2
Dynamic percentage utilization of the adsorptive capacity of the column at 1% [$(C_d(t, L)/C_{d,in}) \cdot 100 = 1\%$]) and 10% [$(C_d(t, L)/C_{d,in}) \cdot 100 = 10\%$)] breakthrough

d_p (m)	d_m (m)	Pe_{intra} (see Eq. 40)	Time at which 1% breakthrough occurs (min)	Time at which 10% breakthrough occurs (min)	Percentage utilization at 1% breakthrough	Percentage utilization at 10% breakthrough
$1.5 \cdot 10^{-5}$	$7.13 \cdot 10^{-8}$	0.0	25.2	48.0	18.440	34.380
		0.035	25.2	48.0	18.440	34.380
		0.1	25.2	48.0	18.440	34.380
		1.0	25.2	48.3	18.440	34.579
		2.0	25.2	48.3	18.440	34.581
		5.0	25.2	48.6	18.441	34.793
		10.0	25.5	50.1	18.661	35.835
		20.0	26.4	56.7	19.322	40.439
		30.0	27.9	71.1	20.425	50.514
		40.0	30.6	80.4	22.407	57.344
		50.0	36.9	87.3	27.011	62.471
		100.0	69.0	106.2	50.546	76.727
		109.0	72.3	108.3	52.966	78.305
		150.0	84.9	114.6	62.224	83.153
$1.5 \cdot 10^{-5}$	$7.13 \cdot 10^{-7}$	0.0	25.2	48.0	18.439	34.376
		0.035	25.2	48.0	18.439	34.376
		0.1	25.2	48.0	18.439	34.376
		1.0	25.2	48.0	18.439	34.377
		2.0	25.2	48.3	18.440	34.577
		5.0	25.2	48.6	18.440	34.789
		10.0	25.5	49.8	18.660	35.633
		20.0	26.1	56.7	19.103	40.437
		30.0	27.9	71.1	20.425	50.511
		40.0	30.6	80.4	22.406	57.340
		50.0	36.6	87.3	26.791	62.467
		100.0	68.4	106.2	50.104	76.719
		109.0	72.0	108.3	52.747	78.300
		150.0	84.9	114.6	62.223	83.148
$1.5 \cdot 10^{-5}$	$7.13 \cdot 10^{-6}$	0.0	18.6	45.3	13.591	32.368
		0.035	18.6	45.3	13.591	32.268
		0.1	18.6	45.3	13.591	32.268
		1.0	18.6	45.3	13.591	32.269
		2.0	18.6	45.6	13.592	32.470
		5.0	18.6	45.9	13.592	32.685
		10.0	18.9	47.4	13.812	33.739
		20.0	20.1	54.9	14.692	38.984
		30.0	22.5	67.2	16.451	47.668
		40.0	26.4	76.5	19.309	54.442
		50.0	33.0	83.1	24.139	59.340
		100.0	60.6	101.1	44.378	72.873
		109.0	63.6	102.9	46.582	74.240
		150.0	75.0	109.2	54.955	79.029

increases as the value of d_m decreases; a significant change occurs as d_m increases from $7.13 \cdot 10^{-8}$ to $7.13 \cdot 10^{-6}$ m. However, it should also be noted by examining the data in Table 2 that the ratios of the dynamic percentage utilizations obtained from increasing values of d_m decrease as Pe_{intra} increases. Consideration of the above observations suggests that the decreases in the dynamic percentage utilization with increasing values of d_m could be reduced by increasing the value of Pe_{intra}. In Fig. 8, the dynamic percentage utilization of the adsorptive capacity of the column at 1% and 10% breakthrough for values of Pe_{intra} from 0 to 150 are presented for $d_m = 7.13 \cdot 10^{-8}$ and $7.13 \cdot 10^{-6}$ m. The results in Fig. 8 indicate that at 1% breakthrough the

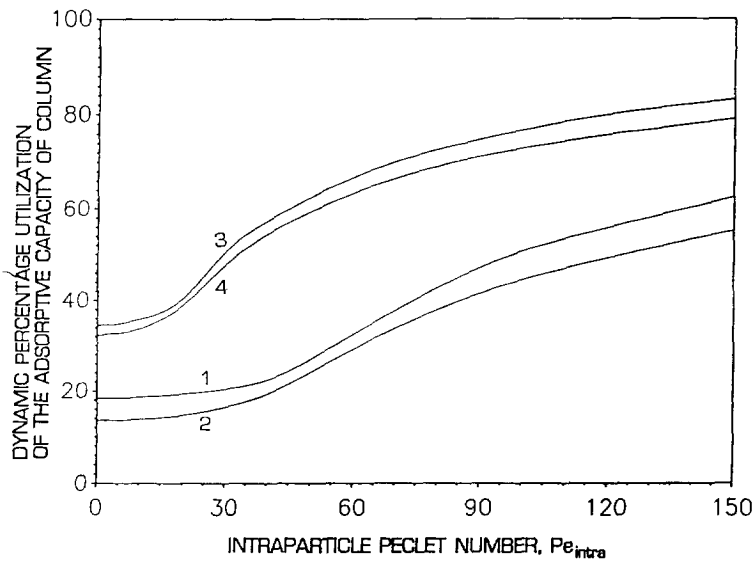

Fig. 8. Dynamic percentage utilization of the adsorptive capacity of column at 1% and 10% breakthrough as a function of intraparticle Peclet number, Pe_{intra}, for $d_m = 7.13 \cdot 10^{-8}$ and $7.13 \cdot 10^{-6}$ m. (1) 1% breakthrough when $d_m = 7.13 \cdot 10^{-8}$ m; (2) 1% breakthrough when $d_m = 7.13 \cdot 10^{-6}$ m; (3) 10% breakthrough when $d_m = 7.13 \cdot 10^{-8}$ m; (4) 10% breakthrough when $d_m = 7.13 \cdot 10^{-6}$ m.

dynamic percentage utilization, for a given d_m value, is similar for Pe_{intra} from 0 to about 20, whereas at 10% breakthrough the dynamic percentage utilization, for a given d_m value, is similar for Pe_{intra} from 0 to about 10. These results suggest that if one plans to switch the column at 1% breakthrough, then a higher dynamic percentage utilization of the adsorptive capacity than that obtained with purely diffusive particles requires that the value of Pe_{intra} of the adsorbent particles should be ≥ 20, and if one plans to switch the column at 10% breakthrough, then the value of Pe_{intra} of the adsorbent particles should be ≥ 10.

4. Conclusions

A mathematical model that could be used to describe adsorption in columns with spherical bidisperse perfusive or spherical bidisperse purely diffusive adsorbent particles was constructed and presented. A numerical solution procedure was also developed and used to solve the unsteady-state spatially multi-dimensional nonlinear partial differential equations of the model. The numerical solution of the mathematical model allows the determination of intraparticle concentration profiles of the adsorbate in the pore fluid and in the adsorbed phase of the spherical bidisperse porous adsorbent particles, the transport rates for a variety of adsorbent particle characteristics and operating conditions of the column and the determination of the concentration of the adsorbate in the flowing fluid stream everywhere in the column including its exit, for intraparticle Peclet numbers ≥ 0.

The dynamic adsorption of BSA on spherical anion-exchange porous particles packed in a column was studied for different values of the intraparticle Peclet number, Pe_{intra}, and of the microparticle diameter, d_m. It was found that the spherical symmetry of the isoconcentration profiles during adsorption inside a porous adsorbent particle, characteristic of purely diffusive porous adsorbent particles, is significantly altered as the magnitude of Pe_{intra} is increased above 2 for the system studied. As Pe_{intra} increases, the smallest concentration of the adsorbate moves downstream, and hence there is higher adsorbate availability in the pore fluid of the macroporous

region and a higher concentration of adsorbate in the adsorbed phase in the upstream than the downstream half of the sphere. Further, as Pe_{intra} increases and the adsorbate concentration minimum moves downstream, the overall adsorbate content of the spherical adsorbent particle increases, and this increases the driving force for mass transfer into the microspheres (microparticles).

It was suggested that if the intraparticle convective velocity could not be measured experimentally for a given kind of chromatographic porous adsorbent particles, then the behavior of the results in Figs. 2–7 could be considered to provide an indirect test for determining if a given kind of chromatographic adsorbent particles could exhibit perfusion behavior when the column is operated under conditions of interest to the user. If, for example, the concentration profiles of the adsorbate molecules in the adsorbed phase of the porous adsorbent particles could be determined experimentally, and if the experimentally determined concentration profiles show a departure from spherical symmetry, then this result could suggest that (considering that the adsorption sites on the surface of the pores were distributed evenly throughout the interior of the adsorbent particles) the porous adsorbent particles of the column may have exhibited perfusion behavior under the conditions of operation of the column.

The dynamic percentage utilization of the adsorptive capacity of the column, for a given value of d_m, increases as Pe_{intra} increases. Further, for a given value of Pe_{intra} the dynamic percentage utilization of the adsorptive capacity of the column increases as the value of d_m decreases. The dynamic percentage utilizations of the adsorptive capacity of the column at 1% and 10% breakthrough, for the system studied here, are increased above that obtained from purely diffusive porous adsorbent particles by increasing Pe_{intra} above 20 and 10, respectively.

Finally, the percentage breakthrough to be selected for column switching is influenced by the value of Pe_{intra} because of its effect on the dynamic percentage utilization of the adsorptive capacity of the column.

Symbols

A	molecule of adsorbate
AS	adsorbate–active site complex
C_d	concentration of adsorbate in the flowing fluid stream of the column (kg/m^3 of bulk fluid)
$C_{d,in}$	concentration of adsorbate at $x<0$ when $D_L \neq 0$, or at $x=0$ when $D_L=0$ (kg/m^3 of bulk fluid)
C_p	concentration of adsorbate in the fluid of the macropores (through-pores) (kg/m^3 of macropore volume)
C_{pm}	concentration of adsorbate in the fluid of the micropores (kg/m^3 of micropore volume)
$\bar{C}_{ps}$	average concentration of adsorbate defined in Eq. 35 (kg/m^3 of perfusive particle)
$\bar{C}_s$	average concentration of adsorbate defined in Eq. 31 (kg/m^3 of microparticle)
$\bar{C}_{sa}$	average concentration of adsorbate in the adsorbed phase defined in Eq. 33 (kg/m^3 of perfusive particle)
C_{sm}	concentration of adsorbate in the adsorbed phase of the microparticle (kg/m^3 of perfusive particle)
C_1	maximum equilibrium concentration of adsorbate in the adsorbed phase of the microparticle (kg/m^3 of perfusive particle)
d_p	diameter of spherical porous adsorbent particle, ($d_p=2R_p$) (m)
D_L	axial dispersion coefficient of adsorbate (m^2/s)
d_m	diameter of spherical microparticle ($d_m=2r_m$) (m)
D_p	effective pore diffusion coefficient of adsorbate in the macropores (through-pores) (m^2/s)
D_{pm}	effective pore diffusion coefficient of adsorbate in the micropores (m^2/s)

$f(C_{pm}, C_{sm}, \boldsymbol{k})$ functional form defined after Eq. 25
F parameter given by Eq. 10
H parameter given by Eq. 11
$\boldsymbol{k}$ vector of adsorption rate constants defined after Eq. 25
k_1 adsorption rate constant in $A + S \underset{k_2}{\overset{k_1}{\rightleftharpoons}} AS$ (m^3 of micropore volume/kg · s)
k_2 adsorption rate constant in $A + S \underset{k_2}{\overset{k_1}{\rightleftharpoons}} AS$ (s^{-1})
K equilibrium adsorption constant of adsorbate, $K = k_1/k_2$ (m^3/kg)
K_p particle permeability (m^2)
L column length (m)
Pe_{intra} intraparticle Peclet number $[Pe_{intra} = (v_{px_1} d_p)/D_p]$ (dimensionless)
r radial distance in microparticle (m)
r_m radius of microparticle (m)
R radial distance in perfusive particle (m)
R_p radius of perfusive particle (m)
S active site
T temperature (K)
t time (s)
$\boldsymbol{v}_p$ intraparticle velocity vector (m/s)
v_{pR} intraparticle velocity component along the R direction (m/s)
$v_{p\theta}$ intraparticle velocity component along the θ direction (m/s)
v_{px_1} axial component of the intraparticle velocity given by Eq. 18 (m/s)
V_f column fluid superficial velocity (m/s)
x axial distance in column (m)
x_1, x_2, x_3 space coordinates of perfusive particle as shown in Fig. 1 (m)

Greek letters

β parameter defined in Eq. 12
ε void fraction in column
ε_p macropore (through-pore) void fraction
ε_{pm} micropore void fraction
η parameter defined in Eq. 13
θ polar coordinate angle (rad)
ξ variable defined in Eq. 9

Acknowledgements

A.I.L. gratefully acknowledges partial support of this work by Monsanto and the NATO Scientific Affairs Division under Grant No. 880770.

References

[1] N.B. Afeyan, N.F. Gordon, I. Mazsaroff, L. Varady, S.P. Fulton, Y.B. Yang and F.E. Regnier, *J. Chromatogr.*, 519 (1990) 1.
[2] A.I. Liapis and M.A. McCoy, *J. Chromatogr.*, 599 (1992) 87.
[3] M.A. McCoy, A.I. Liapis and K.K. Unger, *J. Chromatogr.*, 644 (1993) 1.
[4] A.I. Liapis and M.A. McCoy, *J. Chromatogr. A*, 660 (1994) 85.
[5] A.I. Liapis, *Math. Modelling Sci. Comput.*, 1 (1993) 397.
[6] F.H. Arnold, H.W. Blanch and C.R. Wilke, *Chem. Eng. J.*, 30 (1985) B25.
[7] F.H. Arnold, H.W. Blanch and C.R. Wilke, *Chem. Eng. J.*, 30 (1985) B9.
[8] G. Neale, N. Epstein and W. Nader, *Chem. Eng. Sci.*, 28 (1973) 1865.
[9] M.A. McCoy, *Ph.D. Dissertation*, Department of Chemical Engineering, University of Missouri–Rolla, Rolla, MO, 1992.
[10] A.I. Liapis and K.K. Unger, in G. Street (Editor), *Highly Selective Separations in Biotechnology*, Blackie, Glasgow, 1994.
[11] A.E. Rodrigues, J.C. Lopes, Z.P. Lu, J.M. Loureiro and M.M. Dias, *J. Chromatogr.*, 590 (1992) 93.
[12] B.H. Arve and A.I. Liapis, *AIChE J.*, 33 (1987) 179.
[13] J. Villadsen and M.L. Michelsen, *Solution of Differential Equation Models by Polynomial Approximation*, Prentice-Hall, Englewood Cliffs, NJ, 1978.
[14] C.D. Holland and A.I. Liapis, *Computer Methods for Solving Dynamic Separation Problems*, McGraw-Hill, New York, 1983.
[15] J. Villadsen and J.P. Sorensen, *Chem. Eng. Sci.*, 24 (1969) 1337.
[16] T. Wicks, *Scientific Computing and Analysis Library Report, SCA-LR-52*, Boeing Computer Services, Seattle, 1988.